Available online at www.sciencedirect.com
ScienceDirect
Acta Materialia 58 (2010) 1037–1044
Acta MATERIALIA
www.elsevier.com/locate/actamat

Self-similar grain size distribution in three dimensions: A stochastic treatment

C.S. Pande [a], G.B. McFadden [b,*]

[a] Naval Research Laboratory, Washington, DC 20375, USA
[b] National Institute of Standards and Technology, Gaithersburg, MD 20899, USA

Received 27 July 2009; received in revised form 6 October 2009; accepted 11 October 2009
Available online 13 November 2009

Abstract

In this paper, a stochastic formulation of three-dimensional grain growth is presented. This formulation employs the recent extension of the von Neumann law to three dimensions, and leads to a Fokker–Planck equation for the size distribution. The self-similar solutions of the Fokker–Planck equation presented here are based on the assumption of quasi-stationary distributions reached in the long time limit. The resulting grain size distributions, obtained both numerically and analytically, are shown to be in good agreement with each other and also with those obtained from computer simulations, indicating the validity of the stochastic approach.
Published by Elsevier Ltd. on behalf of Acta Materialia Inc.

Keywords: Grain growth; Modelling; Theory

1. Introduction

Grain growth is a well-known phenomenon in the evolution of material microstructure, resulting in an increase in average grain size by the motion of grain boundaries and the gradual disappearance of the smallest grains during an annealing treatment at a given temperature. An accurate description of the spatial and temporal evolution of a polycrystal from the initial stage, through the transient period, and finally to the quasi-stationary state, is still only poorly understood, especially for three-dimensional (3-D) grain growth. For a review see Ref. [1].

In contrast to 2-D grain growth studies, which have been established on solid foundations due to the existence of von Neumann's law [2] for bubble growth (the validity of which for 2-D grain growth was demonstrated by Mullins [3]), until recently a similar law for 3-D grain growth was lacking. C.S. Smith, commenting on von Neumann's law (see Ref. [2]), stated:

"The discussion by Dr. von Neumann is much appreciated, and his conclusions are as remarkable for their simplicity as they are non-obvious on first consideration of the problem. It is greatly to be hoped that he, or some other mathematician, will be able to deduce similar relations in three dimensions and can combine these with the topological requirements to give the equilibrium distribution of bubbles toward which a froth must tend".

Since then, in recent years a generally accepted law equivalent to von Neumann's law has become available (see Section 2). It is thus appropriate to use it to determine the grain size distribution in three dimensions, at least in the long time limit. It is well-known that in this limit a quasi-stationary state is observed in a wide variety of materials. This state exhibits a scaling property: the grain size distribution (GSD) $F(R, t)$ has an invariant form when expressed in terms of the grain size, R, scaled by its mean value, $\overline{R}(t)$. This is the regime of so-called normal grain growth when only the scale varies with some power of time, the grain size distribution remaining self-similar. These results are true for both 2-D (thin films) and 3-D (bulk) grain growth.

* Corresponding author. Address: National Institute of Standards and Technology, Building 820, Room 365, 100 Bureau Drive Stop 8910, Gaithersburg, MD 20899-8910, USA. Tel.: +1 301 975 2711.
E-mail address: mcfadden@nist.gov (G.B. McFadden).

1359-6454/$36.00 Published by Elsevier Ltd. on behalf of Acta Materialia Inc.
doi:10.1016/j.actamat.2009.10.020

Thus the aim of this paper is to provide explicit numerical and analytical approximations for the grain size distribution in a 3-D metallic system, in the long time limit. (We emphasize that we are concerned here with the scaled self-similar distribution for normal grain growth, in contrast to the actual, unscaled, distribution; see Ref. [1] and the discussion in Section 10.) This is accomplished using the stochastic consideration first given by Pande [5]; see also Refs. [6–9]. (A similar treatment for the 2-D case has been published recently [10,11].) We start by determining the form of the continuity equation for the grain size distribution. For that purpose we need to consider the growth rate of an individual grain in a 3-D ensemble.

2. Growth-rate equation for a 3-D grain

There are now several analytical approaches, based on topological considerations (in particular based on the number of faces or the topological class of the grain), that have been proposed for the growth rate. Mullins [12] took into account the general properties of 3-D grains and derived an expression for the average normalized volume rate of change of grains within a topological class. Later Hilgenfeldt et al. [13] developed a similar relation based on geometrical features of convex bodies, specifically on the caliper radius, which is also related to the mean curvature [14]. This was followed by a similar relation by Glicksman [15,16] based on special polyhedra, which he called "average N-hedra". Finally there is a model [17] that gives the exact volume rate of growth of grains as a function of their particular geometry. MacPherson and Srolovitz [17] (following Cahn [18]) demonstrated that the growth rate could be expressed exactly in terms of $L(D)$, the mean width of the domains, and $e(D)$, the lengths of the triple lines of the grain. For details, the reader is referred to the original papers. In addition, a concise but very clear exposition has been given by Mora et al. [19]. A simplified version, more suitable for our purpose, has been given by MacPherson and Srolovitz [17]:

$$2D_f \frac{d}{dt} D_f = C_1 m\gamma (6 - C_2 f_S^{1/2}), \tag{1}$$

where m is the mobility and γ is the energy of the grain boundary. D_f can be identified with grain size, f_S with the number of surfaces of the grain, and C_1 and C_2 are constants. Taking $f_S = C_3 R^2$ and $D_f = 2R$, where C_3 is another constant and R is equivalent grain size, one obtains:

$$\frac{d}{dt} R = \frac{1}{8} C_1 m\gamma \left(6\frac{1}{R} - C_2\sqrt{C_3} \right). \tag{2}$$

Noting that C_3 has the units of $(\text{length})^{-2}$ leads to the expression:

$$\frac{dR(t)}{dt} = \left\{ \left(\frac{a}{R} - \frac{b}{\overline{R}} \right) \right\}, \tag{3}$$

where a and b are parameters independent of R and t. A very similar equation for dR/dt was obtained by Rios and Glicksman [16] using the topological equation of Glicksman [15]. Our aim here in giving this simplified derivation is to make clear that a relation between R and f is necessary, as was the case in the 2-D case where a relation between R and number of sides was needed in addition to von Neumann's law. Of course by their nature, such relations are only true in a statistical sense.

Eq. (3) leads to an equation for the grain size distribution $F(R, t)$ in the mean field model,

$$\frac{\partial F(R,t)}{\partial t} = \frac{\partial}{\partial R} \left[\left(\frac{a}{R} - \frac{b}{\overline{R}} \right) F(R,t) \right]. \tag{4}$$

This is almost identical to the equation for the grain size distribution first obtained by Hillert [20]. As is well-known, predictions from this treatment are in serious disagreement with experiments. There have been many attempts to improve or modify such models to bring them into agreement with experiments, mostly by modifying the dR/dt term.

There is, however, another problem of a more fundamental nature with the type of continuity given in Eq. (4). Pande and Rajagopal [4] have shown that grain growth models based on a mean-field approach cannot explain many properties of grain growth that are observed experimentally, no matter what form of the growth rate is assumed. They showed that mean field models cannot explain that the long time distribution is independent of the initial distribution. It is well-known that the asymptotic self-similar distribution does not depend on the initial distribution [1]. Mean field models also provide no mechanism to explain scaling of the distribution at large times (self-similarity). These models also need additional constraints (so-called "stability conditions") without which an appropriate distribution cannot be obtained, even in the long time limit. These models also do not provide good justification for these stability conditions. Hence there is a need for a new approach, namely a stochastic treatment.

3. Stochastic effects in grain growth

The continuity Eq. (3) yields a first-order partial differential equation for the size distribution if the growth rate function dR/dt is a single-valued function for all grains of size R at time t. This was assumed by Hillert in deriving an equation similar to Eq. (3). The rationale behind the use of this deterministic growth rate expression is that it will describe the statistical grain growth dynamics adequately if dR/dt is an appropriate average growth rate for all grains of size R in a given state of the system [12]. However, specific grains having the same R value at a given time will have different shapes and possibly different n values, so their growth rates may vary. This fluctuation (or "noise") in the dR/dt function changes the mathematical character of the continuity Eq. (3) significantly.

Pande [5] and Pande and coworkers [5–9,11,12] have attempted to develop a more rigorous theory of isothermal grain growth capable of predicting all of the major attributes of grain growth with minimal assumptions by treat-

ing it as a stochastic process. Mathematically, a stochastic process in its simplest form is described by a function of two variables, one of which is time, and involves both a deterministic term and a random term. Specifically, in this treatment, the relation for dR/dt is retained except that it is noted that it is a statistical relation and not an exact one.

The stochastic continuity, or Fokker–Planck, equation in this case is given by:

$$\frac{\partial F(R,t)}{\partial t} = \frac{\partial}{\partial R}\left\{\left(\frac{a}{R} - \frac{b}{\overline{R}}\right)F(R,t)\right\} + D\frac{\partial F^2(R,t)}{\partial R^2}, \tag{5}$$

where a, b and D are arbitrary parameters independent of R and t that are at this stage yet to be determined. On comparing with the mean field continuity Eq. (4), it is seen that the stochastic version includes an additional expression called the diffusion term. The diffusion term cannot be removed by an averaging procedure as suggested by Mullins [21] since the existence of an averaged quantity (first moment) requires that the second moment that corresponds to the diffusion term must also exist. The magnitude of the diffusion term could, however, be small. This will be one of the issues discussed in this paper, and we leave open the possibility that D could in fact be any value including zero, in which case the treatment will be identical to a mean field treatment. In fact we determine later the value of D from the physics of the problem, using the boundary conditions imposed on the system.

It is difficult to solve Eq. (5) analytically. Our aim in this paper is to solve it approximately in the long time limit, and to compare the results with experiments and computer simulations and also with a solution obtained numerically. For further details regarding the basis for steps leading to Eq. (5), see Refs. [6–9]. The material parameter a can be determined exactly as shown in Ref. [16]. The other two parameters, b and D, can be determined exactly from boundary conditions as shown below. Hence there are no adjustable parameters in Eq. (5), and in our solution presented below.

4. Solution in the long time limit

The continuity Eq. (5) can be recast as an ordinary differential equation by imposing the experimental observation of self-similarity of the grain size distribution [20]. We assume that all grains sizes are accessible and that the total volume (mass) of the polycrystalline system is conserved and finite. Appropriate boundary conditions for the size distribution $F(R, t)$ may thus be written as [5]:

$$F(0,t) = F(\infty,t) = 0. \tag{6}$$

The volume (mass) conservation requirement can be expressed in integral form as:

$$\int_0^\infty R^3 F(R,t)dR = \text{constant}. \tag{7}$$

From the self-similarity condition of the grain size distribution, the spatial and temporal components of $F(R, t)$ can be separated [9] so that it can be expressed as:

$$F(R,t) = t^{-2}f(x), \tag{8}$$

where $x \equiv R/\overline{R}(t)$. Here $\overline{R}$ is defined as the mean (first moment) of the distribution, and it can be shown to vary with time as [1,4]:

$$\overline{R} = 2\lambda t^{1/2}, \tag{9}$$

where λ is a constant. The shape of the renormalized grain size distribution is time invariant but the scale factor $\overline{R}$ increases as the square root of annealing time.

Using Eqs. (8) and (9), Eq. (5) can be rewritten as:

$$\frac{D}{\lambda^2}\frac{d^2f}{dx^2} + \left[\frac{a}{\lambda^2 x} - \frac{b}{\lambda^2} + 2x\right]\frac{df}{dx} + \left[8 - \frac{a}{\lambda^2 x^2}\right]f = 0. \tag{10}$$

As noted above, the parameters λ, D, a and b in the preceding equations are not independent; relationships among them can be determined so that only two parameters appear in the scaled ordinary differential equation (see Eq. (17) below). Letting $\varepsilon = D/\lambda^2$ and $\alpha = b/\lambda^2$, $A = a/\lambda^2$, Eq. (10) is rescaled as:

$$\varepsilon\frac{d^2f}{dx^2} + \left[\frac{A}{x} - \alpha + 2x\right]\frac{df}{dx} + \left[8 - \frac{A}{x^2}\right]f = 0, \tag{11}$$

subject to the boundary conditions $f(0) = f(\infty) = 0$. Eq. (11) can be solved exactly for two limiting cases where the driving force is either due only to the drift velocity (Hillert) or diffusion (Rayleigh).

The Rayleigh grain size distribution occurs when $\alpha = 0$ and $A = 2\varepsilon$. This means that all curvature effects are ignored. The grains during grain growth do a pure random walk in grain size space. Eq. (11) in this case is reduced to:

$$\varepsilon\frac{d^2f_r}{dx^2} + \left[\frac{2\varepsilon}{x} + 2x\right]\frac{df_r}{dx} + \left[8 - \frac{2\varepsilon}{x^2}\right]f_r = 0. \tag{12}$$

This equation can be solved exactly. A solution satisfying all boundary conditions is [9]:

$$f_r(x) = cx\exp\left[\frac{-x^2}{\varepsilon}\right]. \tag{13}$$

The constants c and ε are obtained by requiring the grain size distribution to be normalized and its mean, $\bar{x}$, the first moment of $f_r(x)$, to be equal to unity. This leads to the normalized Rayleigh grain size distribution:

$$f_r(x) = \frac{\pi}{2}x\exp\left[-\frac{\pi x^2}{4}\right]. \tag{14}$$

The Hillert grain size distribution represents the other limiting case, $\varepsilon = 0$, $\alpha = 9$, and $A = 81/8$, which occurs if the drift velocity due to curvature is the only driving force, i.e. the equation is of the first order (mean field). In that case, Eq. (11) reduces to a first-order ordinary differential equation:

$$\left[\frac{(9-4x)^2}{8x}\right]\frac{df_h(x)}{dx} + \left[8 - \frac{81}{8x^2}\right]f_h(x) = 0, \tag{15}$$

the normalized solution of which is [20]:

$$f_h(x) = \frac{34992x}{(9-4x)^5} \exp\left[\frac{-12x}{(9-4x)}\right], \tag{16}$$

for $x \leqslant 9/4$. This distribution is characterized by a finite cut-off at $x = 9/4$. The Rayleigh and Hillert distributions therefore represent limiting cases of the general solution for Eq. (11).

5. Numerical solution

We use the same numerical approach as in our previous treatment [11]. An examination of the first three moments of the differential equation (11) gives an analytical relation between A, ε and α that must hold in order for the solution to have a finite third moment:

$$A = \frac{(2\varepsilon - \alpha^2 - \alpha\varepsilon)}{(1-\alpha)}. \tag{17}$$

See Appendix A for further details. For $\alpha = 0$ this gives $A = 2\ \varepsilon$, in agreement with the Rayleigh distribution. For $\varepsilon = 0$ and $\alpha = 0$ this gives $A = 81/8$, in agreement with the Hillert distribution. If this result is used in the differential equation (11), the numerical solution then determines a further relation between ε and α. Some numerical results are given in Table 1 and in Figs. 1 and 2. Also shown in Fig. 1 is the approximate relation:

$$\varepsilon = \frac{4}{\pi}(1 - \alpha/9)^2, \tag{18}$$

which is seen to be an excellent approximation to the numerical data; the data fall slightly below this curve at the interior points. It appears from the numerical calculation that $\varepsilon = 1$ for $\alpha = 1$, so that the apparent pole at $\alpha = 1$ in Eq. (17) is actually a removable singularity.

Some numerically computed grain size distributions for various values of α are shown in Fig. 3. As α ranges from $\alpha = 0$ to $\alpha = 9$ the distributions vary smoothly, with the peak values increasing and the tails of the distributions become more short-ranged.

6. Estimation of the value of the parameter α

So far in our treatment we have used D, and by implication α, as an independent, adjustable parameter the value of which can be adjusted to obtain a good fit with simulation or experimentally observed grain size distributions. In this section we now show its value can be estimated fairly accurately. For this purpose we note that Rios and Glicksman [16] have shown from topological considerations that

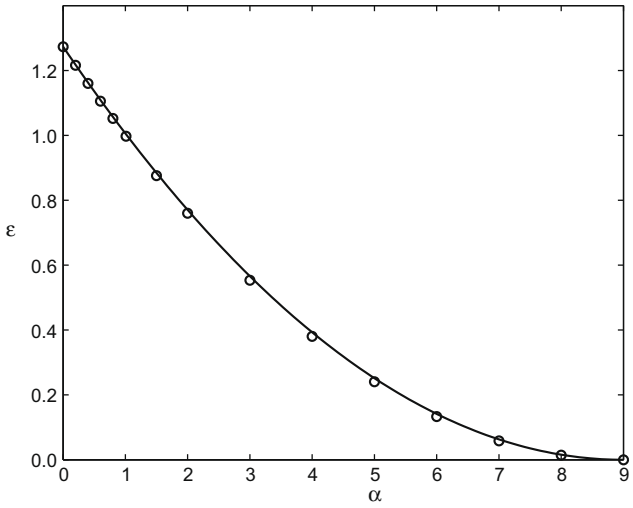

Fig. 1. Numerical determination of ε vs. α (data points), and the approximate relation $\varepsilon = (4/\pi)(1 - \alpha/9)^2$ (curve).

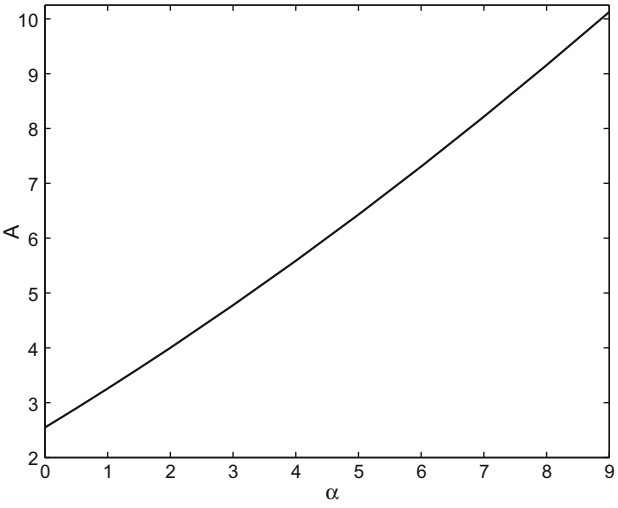

Fig. 2. Numerical determination of A vs. α.

Table 1
Numerical results and approximation errors (see Appendix A for details).

A	ε	p_1	p_2	Δ_2	Δ_1
0.1	1.2444	-2.60619×10^{-2}	0.79665	2.37×10^{-4}	2.59×10^{-4}
0.5	1.1325	−0.13339	0.84321	1.23×10^{-3}	1.44×10^{-3}
1.001	0.99974	−0.27495	0.90509	2.56×10^{-3}	3.29×10^{-3}
2.0	0.75990	−0.58251	1.0413	5.34×10^{-3}	8.40×10^{-3}
3.0	0.55334	−0.92804	1.1967	8.32×10^{-3}	1.59×10^{-2}
4.0	0.38028	−1.3180	1.3750	1.13×10^{-2}	2.63×10^{-2}
5.0	0.24043	−1.7621	1.5808	1.34×10^{-2}	4.06×10^{-2}
6.0	0.13329	−2.2738	1.8212	1.39×10^{-2}	6.28×10^{-2}
7.0	5.81679×10^{-2}	−2.8720	2.1055	1.18×10^{-2}	9.56×10^{-2}
8.0	1.41766×10^{-2}	−3.5833	2.4470	6.04×10^{-3}	0.14
8.5	3.98769×10^{-3}	−3.9956	2.6464	2.64×10^{-3}	0.18

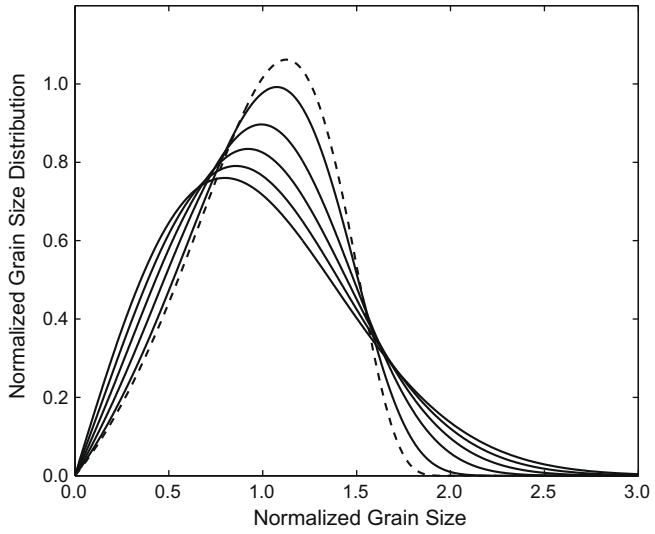

Fig. 3. Numerically computed grain size distributions for, from largest peak to smallest peak, $\alpha = 9$ (Hillert distribution, dashed curve), $\alpha = 8$, $\alpha = 6$, $\alpha = 4$, $\alpha = 2$, and $\alpha = 0$ (Rayleigh distribution).

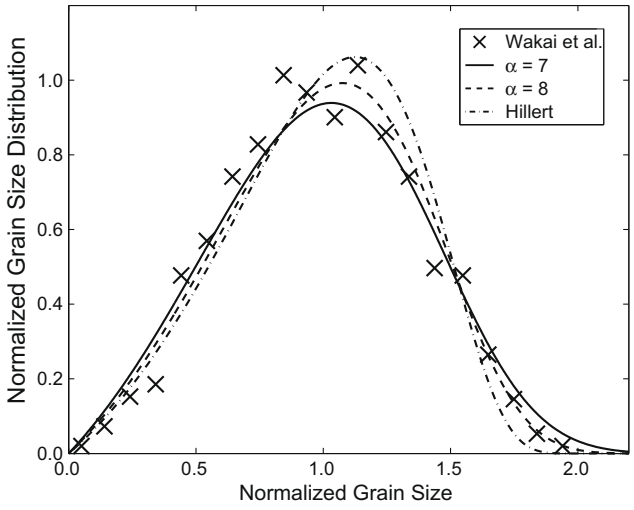

Fig. 4. Comparison of the EVOLVER simulation data of Wakai et al., as depicted by Rios and Glicksman, with the grain size distributions for $\alpha = 7$, $\alpha = 8$, and $\alpha = 9$ (Hillert distribution).

$a = 0.81Gm\gamma$, and Mullins [12] has shown that λ^2 is given by $\lambda^2 = 1/4Gm\gamma$, which gives A as $A = a/\lambda^2 = 0.324/G$. Mullins estimates that G lies between 0.4 and 0.6 with a likely value of 0.5, and is more or less independent of the grain size distribution. A value of $G = 0.5$ gives A as 6.48, which from our calculation corresponds to a value of α about 5. Using the range of G of 0.4–0.6 gives a range of α of 4–7.

Two implications of this result are immediately apparent. First, the GSD is independent of mobility and grain boundary energy, and therefore the GSDs of a variety of materials should have GSDs that are very close to each other; and secondly, the estimated value of α falls almost in the middle of the range, which extends from 0 to 9. GSDs are thus expected to be neither Rayleigh's GSD ($\alpha = 0$) nor Hillert's GSD ($\alpha = 9$) but almost in the middle of this range.

7. Comparison with simulation of Wakai et al. [22]

A comparison with the data of Wakai et al. [22], obtained using the computer program of Brakke [23] (as depicted by Rios and Glicksman [16]) is shown in Fig. 4 for the 3-D GSDs with $\alpha = 7$, $\alpha = 8$ and $\alpha = 9$ (Hillert GSD). The GSD for $\alpha = 8$ apparently does a better job fitting the tail than the other two GSDs. The data of Wakai et al. near the peak are rather noisy and do not easily distinguish the GSDs.

8. Comparison with log-normal distribution

Pande [5], in his survey of early experimental evidence on grain size distributions in a variety of materials, concluded that there is reason to believe that log-normal distribution fits the experimental data fairly well.

The log-normal distribution, defined as:

$$f(x;\mu,\sigma) = \frac{1}{x\sigma\sqrt{2\pi}} \exp\left[\frac{-(\ln x - \mu)^2}{2\sigma^2}\right], \tag{19}$$

for $0 \leqslant x < \infty$, depends on two parameters, μ and σ, which lie in the range $-\infty < \mu < \infty$ and $\sigma > 0$. It has moments given by $\mu_k = \exp[k\mu + k^2\sigma^2/2]$, with a variance $\mu_2 - \mu_1^2 = (\exp[\sigma^2] - 1)\exp[2\mu + \sigma^2]$.

In Fig. 5 we show a comparison of the numerical solution with a log-normal distribution, where μ and σ are determined by fitting the peak of the numerical solution. We take $\alpha = 5$ as this is roughly the expected value of the parameter. The log-normal distribution is flatter for small grain sizes and has a longer tail for large grain sizes.

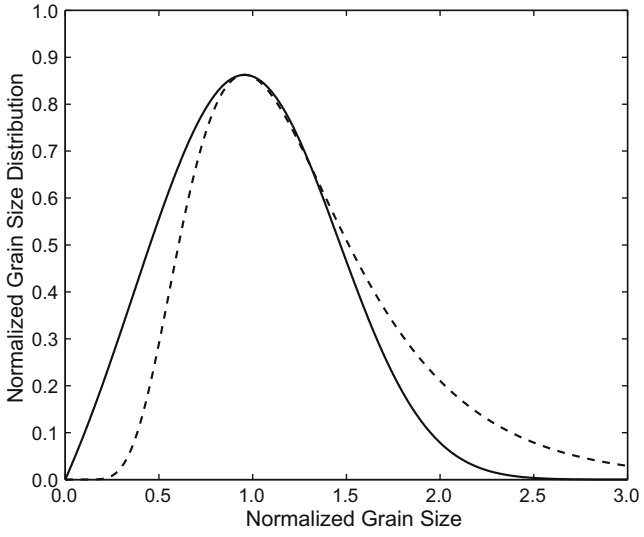

Fig. 5. Comparison of the numerical solution (solid curve) and the log-normal distribution (dashed curve) that has been fitted to the peak of the numerical solution for $\alpha = 5$, using $\mu = 0.148$ and $\sigma = 0.439$.

9. Discussion

In this paper we have considered models of normal grain growth in bulk materials in the long time limit, where appropriately scaled distributions functions with a self-similar form are commonly observed [1]. As such, we neglect the effects of stress, cold-work and recrystallization; these subjects are treated in Refs. [24,25]. In addition, these models neglect effects that are known to alter the kinetics of normal grain growth, such as strongly anisotropic surface energies or mobilities, pinning by defects, or constraints due to finite sample size. For example, Rhines and Patterson [24] found that the grain volume distribution of recrystallized aluminum, determined by separating and weighing the individual grains, was given by a log-normal distribution. The standard deviation of the distribution was found to remain constant during steady-state grain growth, with a value that was dependent on the prior cold-work. Zhang et al. [25] obtained the grain size distribution in recrystallized iron by serial sectioning coupled with quantitative microstructural analysis on 2-D sections. The sampling volume contained approximately 1000 grains. They found that the grain distribution significantly deviated from either log-normal distributions or distributions predicted from mean field theories. These examples illustrate the importance of distinguishing long-term distributions from transient, short-term distributions, and scaled distributions from unscaled distributions, in attempting to make comparisons of normal grain growth theories with experimental observations.

It is interesting to note that an equation similar to our Eq. (45) (see Appendix A) has also been obtained from mean field considerations. The derivation either involves a modification of the growth-rate equation [26] different from that obtained by Hillert, or a modification of the LSW treatment [27]. As stated earlier, a modification of the Hillert equation for the rate of grain growth (except for a large scatter around the growth equation as seen in simulations) is difficult to justify on physical grounds.

As for the treatments involving a modification of LSW method itself, Brown [27] re-examined the classical LSW theory in the context of particle coarsening and concluded that there is an infinite number of quasi-stationary distributions of which the LSW distribution is a particular case. Brown's treatment was improved in the work of Coughlan and Fortes [28]. Essentially the modified LSW treatment gives a family of curves, which, similar to our case, all depend on a single parameter. Rios et al. use this method, for example, in both 2-D [29,30] and 3-D [31] grain growth studies; this approach requires one adjustable parameter and this free parameter can be used to improve Hillert's mean-field approach. It gives a distribution without a theoretical cut-off. Rios et al. [30], however, point out that using a fitting parameter is a "phenomenological" procedure rather than a rigorous solution of the grain growth evolution because for some values of this parameter the distribution does not have a finite cut-off like the Hillert distribution does. This lack of a cut-off is ultimately responsible for divergence of the third moment in that approach; however, the solutions that we present here do have finite third moments.

10. Conclusions

In summary, in this paper we provide solutions to the Fokker–Planck continuity equation for the grain size distribution for 3-D normal grain growth in the long time limit (self-similar state) using the extension of von Neumann's law to three dimensions, together with the stochastic formulation first proposed by Pande [5]. The stochastic formulation of the problem of the grain size distribution considered in this paper, and its solution, is guided by three considerations. First, the result obtained previously by Pande and Rajagopal [4] that for self-similarity a fluctuation term is necessary in the rate equation. Second, that the "strength" of the fluctuation term is limited to a few options; again due to the requirement of self-similarity, the simplest option is a constant independent of time and grain size as is used in the present analysis. Third, that this strength can be estimated by invoking the appropriate boundary conditions (i.e. $F = 0$ at $R = 0$ and $F = 0$ at $R = \infty$), together with the conservation of the specimen volume. This leads us to believe that the source of the fluctuation term may be inherent in these conditions. We show that the "strength" of the diffusion term D can be identified in terms of parameters already determined by Rios and Glicksman [16] and by Mullins [3]. The implication of this result is that although the exact reason for the stochastic behavior may be complicated, the grain size distributions can be obtained precisely without their detailed consideration. The mathematical expressions for the grain size distribution thus obtained have no remaining adjustable parameters, and are in agreement with computational results.

Acknowledgment

This work is supported in part by the Office of Naval Research.

Appendix A

Here we describe in more detail the analysis of the differential equation (11). The point $x = 0$ is a regular singular point for this equation and there is a regular solution having the expansion:

$$f(x) = x + a_2x^2 + a_3x^3 + \cdots + a_nx^n + \cdots, \tag{20}$$

for small x, where:

$$a_2 = \frac{\alpha}{2\varepsilon + A}, \tag{21}$$

and for $n = 1, 2, \ldots$

$$a_{n+2} = \frac{\alpha}{\varepsilon(n+2) + A}a_{n+1} - \frac{(2n+8)}{(n+1)(\varepsilon(n+2) + A)}a_n. \tag{22}$$

The point at infinity is an irregular singularity, and there are solutions with either exponential decay or algebraic decay for large x. The exponentially decaying solutions have the expansion:

$$f(x) \sim e^{-x^2/\varepsilon} e^{\alpha x/\varepsilon} x^{3-A/\varepsilon} w(x), \tag{23}$$

where $w(x)$ represents an asymptotic expansion that tends to a constant for large x:

$$w(x) \sim c_0 + \frac{c_1}{x} + \frac{c_2}{x^2} + \frac{c_3}{x^3} + \cdots, \tag{24}$$

where

$$c_1 = -\frac{3}{2}\alpha c_0, \tag{25}$$

and

$$c_{n+2} = \frac{\alpha(n-2)}{2(n+2)} c_{n+1} - \frac{\varepsilon n^2 + (A-5\varepsilon)n + (6\varepsilon - 3A)}{2(n+2)} c_n. \tag{26}$$

Note that for $\alpha = 0$ and $A = 2\varepsilon$ these expressions give $c_1 = c_2 = 0$, which leads to the (unnormalized) Rayleigh solution:

$$f(x) = x e^{-x^2/\varepsilon}. \tag{27}$$

Algebraically decaying solutions have the formal expansion:

$$f(x) \sim \frac{b_4}{x^4} + \frac{b_5}{x^5} + \cdots, \tag{28}$$

where the coefficients b_n satisfy a recurrence relation of the form:

$$b_5 = 2\alpha b_4, \tag{29}$$

and, for $n = 4, 5, \ldots$

$$b_{n+2} = \frac{\alpha(n+1)}{2(n-2)} b_{n+1} + \frac{(n+1)[\varepsilon n - A]}{2(n-2)} b_n. \tag{30}$$

An example of the latter behavior is the exact solution $f(x) = 1/x^4$ for $\varepsilon = \alpha = A = 0$.

The algebraically decaying solutions do not have a finite third moment, and need to be "filtered" out to obtain the desired solution. This can be affected by the proper choice of the parameters, as we discuss next.

Given the assumed behavior of a solution with $f(x) \sim x + \cdots$ for small x and $f(x) \sim x^{-4} + \cdots$ for large x, we next examine the moments of the ordinary differential Eq. (11). We let μ_k denote the kth moment of the solution:

$$\mu_k = \int_0^\infty x^k f(x) dx, \tag{31}$$

for $k = 0, 1, 2, \ldots$ The first three moments of the ODE are given by:

$$-A\mu_{-1} + \alpha\mu_0 + 4\mu_1 = 0, \tag{32}$$

$$(2\varepsilon - 2A)\mu_0 + 2\alpha\mu_1 + 2\mu_2 = 0, \tag{33}$$

$$(6\varepsilon - 3A)\mu_1 + 3\alpha\mu_2 + 2\lim_{x\to\infty} x^4 f(x) = 0, \tag{34}$$

respectively. Assuming that we have normalized the solution so that $\bar{x} = 1$ implies that $\mu_1 = \mu_0$, and allows us to express the second moment in Eq. (33) as:

$$\mu_2 = (A - \varepsilon - \alpha)\mu_0. \tag{35}$$

From Eq. (34) we then have:

$$[(6\varepsilon - 3A) + 3\alpha(A - \varepsilon - \alpha)]\mu_0 = -2\lim_{x\to\infty} x^4 f(x). \tag{36}$$

The choice $(6\varepsilon - 3A) + 3\alpha(A - \varepsilon - \alpha) = 0$ thus ensures that the solution component with a divergent third moment is eliminated, so that $x^4 f(x) \to 0$ as $x \to \infty$; this produces the relation given in Eq. (17).

We now determine two useful approximations to the grain size distribution in the long time limit. Most grain size distributions for grain growth appear to have characteristics common to a Rayleigh distribution, e.g. a large and broad shape with a single peak and a long tail. Thus we first consider an analytical approximation of the form:

$$f_1(x) = Kx \exp(-p_1 x - p_2 x^2), \tag{37}$$

where the constants p_1 and p_2 will be determined in terms of ε, α and A. An integration shows that the normalizing pre-factor K is given in terms of p_1 and p_2 by:

$$K = \frac{2p_2}{1 - \sqrt{\pi}\xi \exp(\xi^2)\mathrm{erfc}(\xi)}, \quad \xi = \frac{p_1}{2\sqrt{p_2}}, \tag{38}$$

where

$$\mathrm{erfc}(y) = \frac{2}{\sqrt{\pi}} \int_y^\infty \exp[-y^2] dy, \tag{39}$$

is the complementary error function. To develop expressions for p_1 and p_2 we compare moments for the exact and approximate solutions. The moments

$$I_n = \int_0^\infty x^n f_1(x) dx, \tag{40}$$

are found to satisfy the general recurrence relation $2p_2 I_n + p_1 I_{n-1} - n I_{n-2} = 0$ for $n \geqslant 1$, giving:

$$2p_2 I_1 + p_1 I_0 - I_{-1} = 0, \quad 2p_2 I_2 + p_1 I_1 - 2I_0 = 0.$$

Comparing these expressions with the analogous relations (32) and (33) for the exact solution, with the normalizations $I_1 = I_0$ and $\mu_1 = \mu_0$,gives:

$$I_{-1}/I_0 = 2p_2 + p_1, \quad \mu_{-1}/\mu_0 = (4+\alpha)/A,$$

$$I_2/I_0 = (2 - p_1)/2p_2, \quad \mu_2/\mu_0 = A - \varepsilon - \alpha.$$

Setting $I_{-1}/I_0 = \mu_{-1}/\mu_0$ and $I_2/I_0 = \mu_2/\mu_0$ and solving for p_1 and p_2 then gives

$$p_1 = \frac{(4+\alpha)(\varepsilon+\alpha) - A(2+\alpha)}{A(1 - A + \varepsilon + \alpha)},$$

$$p_2 = \frac{(4+\alpha) - 2A}{2A(1 - A + \varepsilon + \alpha)}. \tag{41}$$

To utilize these expressions a relationship between α and ε is required. As was shown earlier, a convenient and excellent fit to the numerically determined relationship between α and ε is given by Eq. (18).

Thus for any given α, the approximate GSD given by Eq. (37) can be determined. We expect a good fit for small values of α, since Eq. (37) recovers the Rayleigh GSD

exactly for $\alpha = 0$. For values of α closer to $\alpha = 9$ we find that this approximation is inaccurate (numerical examples are given below), so we next consider an improved approximation in this limit.

To do so, we approximate the second derivative term in Eq. (11) by writing

$$\frac{d^2 f(x)}{dx^2} = \frac{d}{dx}\left[\frac{df(x)}{dx}\right] = \frac{d}{dx}\left[\frac{d\{\ln[f(x)]\}}{dx} f(x)\right]. \tag{42}$$

Now if $h(x)$ is a good approximation to $f(x)$ we may replace $\ell n\{f(x)\}$ by $\ell n\{h(x)\}$ in this expression. Using our previous approximation, $h(x) = f_1(x)$, this gives the approximate equation:

$$\left[\frac{d}{dx}\left[\left(\varepsilon\frac{d\{\ln[f_1(x)]\}}{dx} + \frac{A}{x} - \alpha + 2x\right) f(x)\right]\right] + 6f(x) = 0. \tag{43}$$

The second-order ordinary differential equation has thus been reduced to first order and now can be integrated immediately. Note that since we have only approximated the second derivative term, for $\varepsilon = 0$ the solution to the approximate equation will reproduce the Hillert GSD exactly. In addition, since $f_1(x)$ is an exact approximation for $\alpha = 0$, the solution of (43) reproduces the Rayleigh GSD exactly as well. From Eq. (37) we find the relatively simple form:

$$\frac{\mathrm{d}[\ln(f_1)]}{\mathrm{d}x} = \frac{1}{x} - p_1 - 2xp_2, \tag{44}$$

and the solution to Eq. (43) is found to have the form:

$$f_2(x) = \frac{6\bar{a}^{3/\bar{b}}}{(\bar{a} + \bar{c}x + \bar{b}x^2)^{(3+\bar{b})/\bar{b}}} x \times \exp\left\{\frac{6\bar{c}}{\bar{b}\Delta}\tan^{-1}\left[\frac{\bar{c} + 2\bar{b}x}{\Delta}\right] - \frac{6\bar{c}}{\bar{b}\Delta}\tan^{-1}\left[\frac{\bar{c}}{\Delta}\right]\right\}, \tag{45}$$

where

$$\bar{a} = A + \varepsilon, \quad \bar{b} = 2 - 2\varepsilon p_2, \quad \bar{c} = -\alpha - \varepsilon p_1, \quad \Delta = \sqrt{4\bar{a}\bar{b} - \bar{c}^2}. \tag{46}$$

A comparison of the numerical GSD and the two approximations for $\alpha = 8$ is shown in Fig. 6. The numerical solution (open circles) and the approximation $f_2(x)$ agree to graphical accuracy, while the approximation $f_1(x)$ has a peak that is noticeably shifted to smaller radii. In Table 1 we give some numerical results for the maximum absolute error Δ_2 between the numerical solution and $f_2(x)$, and for the maximum absolute error Δ_1 between the numerical solution and $f_1(x)$, over the interval $0 < x < 3$, for various values of α. The numerical solution is computed to high accuracy, and can be considered to be exact for these comparisons. Both $f_1(x)$ and $f_2(x)$ are good approximations for small values of α, but $f_1(x)$ becomes increasingly inaccurate as α increases, whereas $f_2(x)$ is also a good approximation as α approaches 9. The largest error in approximation $f_2(x)$ occurs near $\alpha = 6$, with an error of 1.4%.

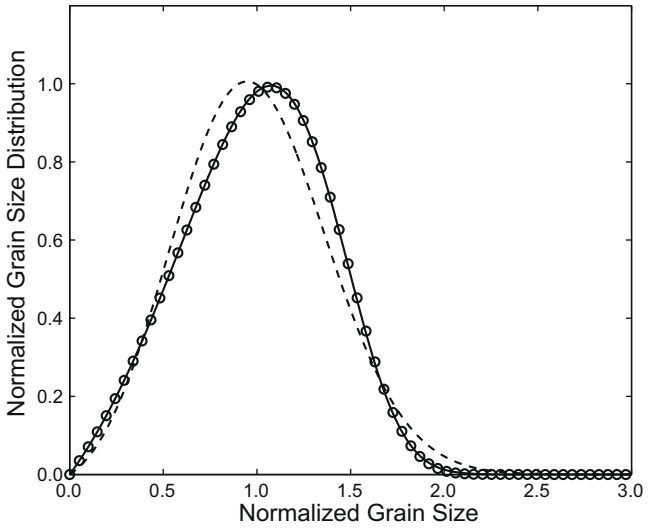

Fig. 6. Comparison of the numerical solution (data points), the approximation $f_1(x)$ from Eq. (37) (dashed curve), and the approximation $f_2(x)$ from Eq. (45) (solid curve), for $\alpha = 8$.

References

[1] Atkinson HV. Acta Metall 1988;36:469.
[2] von Neumann J. In: Metal Interfaces. Cleveland, OH: American Society for Metals; 1952. p. 108.
[3] Mullins WW. J Appl Phys 1956;27:900.
[4] Pande CS, Rajagopal AK. Acta mater 2001;49:1805.
[5] Pande CS. Acta Metall 1987;11:2671.
[6] Pande CS, Dantsker E. Acta Metall 1990;38:945.
[7] Pande CS, Dantsker E. Acta Metall 1991;39:1359.
[8] Pande CS, Dantsker E. Acta Metall 1994;42:2899.
[9] Pande CS, Masumura RA, Marsh SP. Phil Mag A 2001;81:1229.
[10] Pande CS, Cooper KP. Acta Mater 2008;56:4200.
[11] Pande CS, Cooper KP, McFadden GB. Acta Mater 2008;56:4304.
[12] Mullins WW. Acta Metall 1989;37:2979.
[13] Hilgenfeldt S, Krynik AM, Koehler SS, Stone HA. Phys Rev Lett 2001;6:2685.
[14] Minkowski H. Math Ann 1903;57:447.
[15] Glicksman ME. Phil Mag 2005;85:3.
[16] Rios PR, Glicksman ME. Acta Mater 2008;56:1165.
[17] MacPherson RD, Srolovitz DJ. Nature 2007;446:1053.
[18] Cahn JW. Trans Met Soc AIME 1967;239:610.
[19] Barrales Mora LA, Mohles V, Shvindlerman LS, Gottstein G. Acta Mater 2008;56:1151.
[20] Hillert M. Acta Metall 1965;13:227.
[21] Mullins WW. Acta Mater 1998;46:6219.
[22] Wakai F, Enomoto N, Ogawa H. Acta Mater 2000;48:1297.
[23] Brakke KA. Exp Math 1992;1:141.
[24] Rhines FN, Patterson BR. Metall Trans A 1982;13:985.
[25] Zhang C, Suzuki A, Ishimaru T, Enomoto M. Metall Mater Trans A 2004;35:1927.
[26] Zöllner D, Streitenberger P. Scripta Mater 2006;54:1697.
[27] Brown LC. Acta Metall 1989;37:71.
[28] Coughlan SD, Fortes MA. Scripta Metall Mater 1993;28:1471.
[29] Rios PR. Scripta Mater 1999;40:665.
[30] Rios PR, Lücke K. Scripta Mater 2001;44:2471.
[31] Rios PR, Dalpian TG, Brandao VS, Castro JA, Oliveira ACL. Scripta Mater 2006;54:1633.